An Experiment to Measure $\Delta\sigma_{Tot}$ in p-p and $\bar{p}$-p Scattering Between 100 and 500 GeV

D. Hill, H. Spinka, K. Toshioka, D. Underwood, R. Wagner and A. Yokosawa
Argonne National Laboratory, Argonne, Illinois

Y. Hemmi, K. Imai, R. Kikuchi, K. Miyake, T. Nakamura,
K. Nishimura and N. Tamura
Kyoto University, Kyoto, Japan

H. Azaïez, K. Kuroda, A. Michalowicz, D. Perret-Gallix
LAPP, Annecy, France

G. Shapiro
Lawrence Berkeley Laboraotry
University of California, Berkeley, California

D. H. Miller and C. LeRoy
Northwestern University, Evanston, Illinois

M. Corcoran, H. E. Miettinen, T. A. Mulera, G. S. Mutchler,
G. C. Phillips and J. B. Roberts
Rice University, Houston, Texas

J. Bistrisky and F. Lehar
Saclay, France

R. Birsa, F. Bradamante, S. Dalla Torre-Colautti, M. Giorgi, L. Lanceri,
A. Martin, P. Moras, A. Penzo, P. Schiavon and A. Villari
INFN, Sezione di Trieste, Trieste, Italy

Scientific Spokesman:
G. Shapiro
Lawrence Berkeley Laboratory
FTS: 451-6802
Commercial: (415) 486-6802

January 27, 1981

ABSTRACT

It is proposed to measure $\Delta\sigma_L^{Tot}$, the difference in total cross-section between states polarized parallel and anti-parallel, in proton-proton and proton-antiproton scattering between 100 and 500 GeV, using the Fermilab polarized proton/antiproton beam incident on a polarized proton target. This proposal deals only with polarizations along the beam direction, but an obvious rearrangement of the experimental components allows measurements of $\Delta\sigma_T^{Tot}$, involving transverse polarization.

Introduction

We propose to measure the total cross-section difference, in pp and $\bar{p}p$ interactions, between the states with polarization of target and beam aligned parallel and anti-parallel.

This is a straightforward experiment, making use of the polarized beam at FNAL, to explore the spin-dependence of particle interactions at energies in the 100 to 500 GeV range. There are already several experimental indications that spin effects are significant at high energies. Hyperons produced inclusively in proton-nucleus collisions are observed to have high polarizations.[1] Spin-correlation parameters, at the highest energies at which they have been measured, are seen to have large values.[2] We are led to expect that spin-dependent total cross-section differences may persist into the region of Fermilab energies. The unpolarized total cross-section in pp

scattering rises by a few millibarns in this energy range, and we are interested in the extent to which the helicity changing amplitudes participate in this rise. In any case the spin-dependent cross sections in this energy range are almost completely terra incognita at this stage. With the capabilities now in hand to explore the region, these measurements should be made.

In proton- anti-proton interactions there are good physical reasons to expect polarization effects at the highest energies. In any process involving the annihilation of spin - $\frac{1}{2}$ particles, at energies such that their mass can be neglected, into vector intermediate states (e.g., electron-positron pairs forming virtual photons or weak bosons, or quark-antiquark annihilating into vector gluons) a reaction with the initial particles having like helicities is almost completely suppressed (by a factor γ) relative to the rate for the same reaction in states with opposing helicities. This means that, according to any constituent model of hadrons, the longitudinal spin-dependence of any process dominated by such parton annihilations should approach the maximum. We understand that in any real process the efect will be reduced because 1) not all reactions involve annihilation (the $\bar{p}p$ total cross-section at 100 GeV is still 10% higher than that of pp, as an indication), and 2) the polarization of the quarks in a proton is less than that of the proton itself (one naively expects the quarks, on average, to have one-third the proton polarization, but this factor varies depending on the kinematic parameters). Nevertheless we use this illustration as an argument that theories of particle physics do not necessarily predict zero polarization effects at high energies.

Experimental Setup

This experiment will be a standard transmission experiment with the detectors specially designed for a high-divergence beam.

The layout of the experimental setup is shown in Figure 1. A polarized proton or anti-proton beam, which is to be constructed in the M-2 beam line, entering from the left passes through a threshold Cherenkov counter (C_1) set to reject pions, then through four scintillator-hodoscope planes (HX_1, HY_1, HX_2, HY_2) and interacts with a polarized proton target. The unscattered beam and forward scattered particles pass through six scintillator-hodoscopes (HX_3, HY_3, HX_4, HY_4, HX_5, HY_5). The anticoincidence counters A define the useful beam. The counter-hodoscopes IC help in the identification of inelastic events. Another threshold Cherenkov counter (C_2) rejects pions in the final state.

It seems likely that the hodoscopes used in this experiment will share some elements in common with those used to support the scintillator-target polarimeter[3] which measures the polarization of the beam, using elastic scattering in the Coulomb interference region. With a longitudinally polarized beam, of course, the polarimeter cannot monitor the beam polarization directly during the actual experiment, and so there is no conflict in using the same apparatus for both purposes.

Polarized Beam

The beam is described in FNAL proposal A-581. Polarized protons and anti-protons are derived from the parity-violating decay of lambda particles. Either sign of transversely polarized protons can be selected, and

alternated from spill to spill, by the tuning of a vernier magnet upstream of the beam-defining collimators. The beam is transported without loss of polarization to the experimental area. A sequence of eight dipole magnets serves to rotate the spin into the longitudinal direction without altering the direction of the beam or causing any net lateral displacement.

With a momentum bite of ± 5% (rms) and an angular divergence of one milliradian (rms), we expect to obtain a beam intensity of 3×10^7 polarized protons per spill, for 10^{13} protons incident. The beam polarization is expected to be between 40% and 50%. The proton intensity varies slightly with energy, as shown in Figure 2.

The intensity of the polarized antiproton beam has a maximum of about 5×10^6 per spill at an energy in the region of 150 to 200 GeV. We will select the exact energy for our measurement of $\Delta\sigma_L^{Tot}$ in $\bar{p}p$ scattering after survey of the constructed beam shows us where the peak intensity lies. This beam is likewise expected to have between 40% and 50% polarization.

Polarized Target

We will use a standard polarized proton target, polarized longitudinally in a superconducting solenoid magnet. A target material such as ethylene glycol or propanediol, 10% hydrogen by weight and with a free proton density of .07 gm/cm^3, can be used to reliably obtain target polarization above 80%. More exotic materials, such as solid NH_3, have been investigated because of their higher fractional hydrogen content, and may be used if the state of the art warrants it at run time.

The target will be 10 centimeters long, with a diameter transverse to the beam of 2.5 cm.

Scintillation-Counter Hodoscopes

Schematic diagrams of the HX1 and HY1 planes are shown in Figure 3. Each X- and Y-plane (i) consists of an array of N_i scintillation-counters 5 mm thick x W_i mm wide. Both planes are placed parallel to each other and the center beam line passes perpendicularly through their centers. Whenever a beam or forward-scattered particle passes through a hodoscope-pair, it is almost always counted by only one X and one Y scintillation counter. The light from both ends of each counter is fed via two fiberglass lightguides to the corresponding photomultiplier device.

Table I: Scintillator-Hodoscopes

i	N_i	Counter Width W_i (mm)	Hodoscope Width $N_i W_i$ (mm)	Target to Hodoscope Distance Z_i (meters)
1	20	1.5	30	-9.0
2	20	1.0	20	-0.2
3	20	1.5	30	1.0
4	30	1.5	45	9.0
5	45	1.5	68	18.0

Trigger Requirements and Data Collection

The two pairs of beam hodoscopes (see Figure 1) will be used to define the direction of incidental protons or antiprotons.

The beam hodoscope logic will reject ambiguous or multi-particle incident tracks. In addition the Cherenkov counter, upstream of the beam hodoscopes and of the 8-magnet spin precession system, will veto charged pions present in the beam. The anticoincidence counters A will be used to insure that only beam particles that potentially pass through the whole length of the target are in the trigger. The matrix logic will further refine this condition.

The primary function of downstream hodoscopes is to define the angles and positions of the outgoing particles. The presence of the three pairs of hodoscopes will provide sufficient redundancy to permit the continuous monitoring of the individual hodoscope elements. The comparison of the hodoscope hit patterns upstream and downstream of the target will provide an additional check on the continuity of the beam and scattered particle tracks through the target.

The electronic hardware will provide sufficient flexibility to either reject multi-particle events entirely, thus selecting elastic or low-multiplicity events, or to identify the leading particle track (more precisely the track with the minimum scattering angle).

To simplify the logic we plan to process the signals generated by the X and Y arrays separately. This method lends itself more naturally to the use of the projected angles θ_X and θ_Y and not to the polar angle θ ($\theta^2 = \theta_X^2 +$

θ_y^2). From the incident and outgoing angles (projected) the scattered angles will be calculated by hardware. After each event the appropriate scalars associated with the incident and outgoing angles and positions will be incremented. At this stage we use the hardware to combine θ_x, θ_y and increment the scaler corresponding to the polar angle θ. The θ-distributions of opposite incident-proton spin-directions will serve to eliminate elastic scattering background.

These as well as the other scalers will be read into an on-line computer at least once for each spill. In addition, magnet currents, target polarization and hodoscope hit-patterns will periodically be sampled and read into the computer in order to monitor various experimental parameters such as beam profiles and phase space.

We would like to emphasize that since this is a scaler experiment and since beam polarization flips every alternate spin, it is relatively easy to obtain $\Delta\sigma_L$ values on-line.

Trigger Logic and Electronics Requirements

To measure a total cross-section, we must count all incident tracks within the live time of the apparatus. A transmitted particle is defined by the following 5 requirements.

T_0 - Neither the incident, nor the most forward track should be a pion.

T_1 = One and only one incident track in each x and y-plane.

T_2 = The incident track must lie within the range of the angular beam-divergence, and pass through the target.

T_3 = Only one outgoing scattering track in H4 and H5 or both.

T_4 = The most forward scattering track must match with the incident track at the target within the spatial resolution of the hodoscope-system.

We scale all beam tracks, outgoing tracks, and their matrix-coincidences. We scale separately coincidences with only 1 hit in H3 and coincidences with multiple hits in H3 and/or hits in IC1 and IC2.

The high rate of about 3×10^7 particles/spill (of 20 seconds) in each hodoscope, poses rather stringent constraints on the electronic logic's time resolution and speed. We estimate that we need approximately a speed of 30 - 100 nsec. To be able to distinguish particles from different RF-buckets, we need a maximum of 15 nsec in time resolution.

We plan to use standard electronic logic with matrices to perform all the required functions. In Table II we list the electronic circuitry to be used for most of these functions.

Table II

Function	Electronic Circuit
N_i	Digital Adder
$\Sigma X_i < 1$	Analog Linear Add
Minimum (A, B, C,...)	Matrix + "And"
θ_x^2, θ_y^2	Matrix
Δx	Matrix

In Figure 4 we sketch the implementation of some of the above functions.

$\Delta\sigma_L$ Measurement

The amount of beam passing through the polarized-proton target is attenuated by both the free polarized protons and by the rest of the material in the target. The number of particles, N_i (corrected for efficiency), that is transmitted through the target into the ith solid angle covered by segments of the transmission hodoscope is give by:

$$N_i^{\pm} = N_0^{\pm} \exp\left[-\alpha_i - \frac{1}{A}\left(\sigma_i \pm P_B P_T \frac{\Delta\sigma_{L,i}}{2}\right)\right], \qquad (1)$$

where $\pm$ refers to the beam and target polarization oriented antiparallel (+) or parallel (-), N_0 is the number of incident beam particles, α_i is an attenuation constant for everything in the target except free hydrogen, σ_i is the integrated differential cross section from the ith solid angle subtended, $A = (N_A \rho_F L)^{-1} = 2320$ mb is the target constant for free hydrogen, N_A is Avogadro's number, $\rho_F = 0.0714$ gm/cm^3 is the free-proton density, $L = 10$ cm is the target length, and $P_B = 0.5$ and $P_T = 0.8$ are the magnitude of the beam and target polarizations, respectively.

The partial cross-section difference for each counter, $\Delta\sigma_{L,i}$, is calculated from these numbers by:

$$\tanh \frac{\Delta\sigma_{L,i} P_B P_T}{2A} = - \frac{N_i^+/N_0^+ - N_i^-/N_0^-}{N_i^+/N_0^+ + N_i^-/N_0^-} \quad . \qquad (2)$$

In Figure 4 we sketch the implementation of some of the above functions.

$\Delta\sigma_L$ Measurement

The amount of beam passing through the polarized-proton target is attenuated by both the free polarized protons and by the rest of the material in the target. The number of particles, N_i (corrected for efficiency), that is transmitted through the target into the ith solid angle covered by segments of the transmission hodoscope is give by:

$$N_i^{\pm} = N_0^{\pm} \exp\left[-\alpha_i - \frac{1}{A}\left(\sigma_i \pm P_B P_T \frac{\Delta\sigma_{L,i}}{2}\right)\right], \qquad (1)$$

where $\pm$ refers to the beam and target polarization oriented antiparallel (+) or parallel (-), N_0 is the number of incident beam particles, α_i is an attenuation constant for everything in the target except free hydrogen, σ_i is the integrated differential cross section from the ith solid angle subtended, $A = (N_A \rho_F L)^{-1} = 2320$ mb is the target constant for free hydrogen, N_A is Avogadro's number, $\rho_F = 0.0714$ gm/cm^3 is the free-proton density, $L = 10$ cm is the target length, and $P_B = 0.5$ and $P_T = 0.8$ are the magnitude of the beam and target polarizations, respectively.

The partial cross-section difference for each counter, $\Delta\sigma_{L,i}$, is calculated from these numbers by:

$$\tanh \frac{\Delta\sigma_{L,i} P_B P_T}{2A} = - \frac{N_i^+/N_0^+ - N_i^-/N_0^-}{N_i^+/N_0^+ + N_i^-/N_0^-} \quad . \qquad (2)$$

Note that the dominant contributions to the attenuation, α_i and σ_i/A, exactly cancel in this expression. The efficiencies also cancel to first order because the beam polarization is flipped on alternate pulses.

Rates and Run Plan

The statistical accuracy of the $\Delta\sigma_L$ measurement is expressed by

$$\Delta(\Delta\sigma_L) = \frac{2A}{P_B P_T} \left(\frac{1-T}{T}\right)^{1/2} \frac{1}{N_0}$$

where T is the fraction of the beam transmitted by the entire target. For this target T is about .15. With the given values of these parameters, we have

$$\Delta(\Delta\sigma_L) = 4800 \text{ mb}/\sqrt{N_0}$$

Our experience shows us that we can easily achieve an accuracy of ± 100 microbarns, with the techniques used in previous experiments.[4] We feel that with proper care it is reasonable to aim for an accuracy of ± 10 microbarns. This level of precision will be necessary especially if the measured effects turn out to be small.

This means that we will need 2×10^{11} incident protons for each energy data point. At 3×10^7 protons per spill every 50 seconds, this translates into 100 hours of data-taking.

We request 100 hours of beam for each of five energies between 100 and 500 GeV of proton-proton scattering. We also will need 100 hours for checking out the geometry of the experiment to reduce systematic errors.

For the anti-proton beam, with its lower intensity, we cannot achieve the same level of statistical accuracy. We ask for 200 hours of beam time, which will include both checking-out and data-taking. We will run at the energy which our survey shows yields the maximum anti-proton intensity (expected to lie between 100 and 200 GeV).

The total request is thus for 800 hours.

An obvious extension of this experiment is to measure the total cross-section difference $\Delta\sigma_T^{Tot}$ for transversely polarized beam and target. The changes required are to alter the spin-precession magnets to yield transverse beam polarization, and to rotate or substitute the polarized-target magnet so that the field is transverse to the beam. The rest of the apparatus, and the manner of data-taking is unchanged, as are the error and time estimates. Some systematic effects are introduced by the fact that beam and scattered particles are slightly deflected by the polarized-target magnet field, but these are not expected to cause any serious problems.

Systematic Errors

Experients with polarized beams and polarized targets, in which the polarization of each is reversed frequently, have the happy property of cancelling out many kinds of systematic errors. Sources of -- for example, detector inefficiencies, or geometrical misalignments -- which change slowly with respect to the period of polarization reversal, have little effect on the value of the parameters measured by the experiment.

The systematic errors that are correlated with the beam or target polarization can be classified as multiplicative or additive. The multiplicative errors refer to those factors by which the raw asymmetry must be multiplied, or divided, to yield the final result. When the asymmetry is small, and the number of counts are so few that statistical errors dominate, multiplicative errors may not be important.

Additive errors, which can introduce a spurious asymmetry into the data, are more serious. In the case where both beam and target are polarized, and reversed at independent intervals, each type of polarization can be used to monitor, and to cancel out, additive errors associated with the other polarization.

The following kinds of systematic error are common to most polarization experiments:

1) Target polarization measurement (multiplicative error associated with polarized target). The polarization of the target can be measured to an accuracy of ± 3%. The principal uncertainties lie in the calibration of the nuclear magnetic resonance system, using the (small) thermal equilibrium signal. Other uncertainties are introduced by non-linearities in the measuring system when the polarization becomes very large.

2) Beam polarization measurement (multiplicative factor associated with polarized beam). The beam polarization will be measured using the scintillation-target polarimeter[3], designed by members of this group, based on elastic scattering in the Coulomb interference

region. Beam polarization will be measured in the same configuration (and possibly using some of the same counters) with transverse polarization. The spin will then be rotated to the longitudinal orientation, and the polarimeter can be used to verify that no transverse components remain.

It is estimated that the calculation of beam polarization based on beam kinematics is probably accurate to ± 3%.

3) Change in beam geometry with beam polarization (additive factor associated with beam). We control this source of error by
   (a) using the 8-magnet spin reversal scheme that maintains constant geometry.
   (b) doing polarization reversal upstream of the collimator
   (c) using the incident beam telescope, and matrix coincidence to define aceptable incident beam direction.
   (d) Comparing asymmetries observed with the two senses of target polarization. We also check that we get a null effect when target is unpolarized.

In the total cross-section measurement there is an additional source of systematic error because, in a transmission geometry, the quantity measured is the total cross-section <u>minus</u> the cross-section for elastic scattering into the solid angle unresolvable by the detector (about .1 milliradian in this design). The latter cross-section is a fraction of a millibarm at the energies considered here. To estimate the contamination, we can measure the angular dependence of the elastic cross-section in the two spin states using

the diagnostic data from these scattering events sampled by the computer.

We expect to make careful monitoring of accidental rates, and of the efficiencies of the counters as the data is being gathered.

Apparatus

1) Use of one of the existing Argonne polarized proton targets.
2) Threshold Cherenkov upstream to reject incident pions.
3) Threshold Cherenkov downstream to reject events in which fast pions are produced.
4) Ten scintillator hodoscopes, five horizontal and five vertical whose characteristics are given in Table II.
5) Fast hard-wired matrix coincidence logic, with 15 ns time resolution, to perform the following functions for each event triggering the experiment.
   (a) Veto any event in which more than one scintillator has a count in any of the upstream hodoscopes.
   (b) Define trajectories that will intersect the polarized target.
   (c) Measure $(x,y)^{(in)}$ and $(x,y)^{(out)}$ - coordinates and (θ_x, θ_y) angles of these trajectories.
   (d) Calculate $\theta^2 = \theta_x^2 + \theta_y^2$.
   (e) Measure number of hits in each hodoscope $(N^{(i)})$.
6) Fast scalers, gated for live-time (plus some ungated ones) to count:
   (a) Incident protons.

(b) Events from x- and y-hodoscopes.

(c) Events from the matrix coincidence logic.

7) Monitor telescope.

8) On-line computer to perform the following functions:

(a) Control and measure target polarization.

(b) Record all scalars and monitors, one per spill.

(c) Various on-line diagnostics.

References

1. K. Heller et al., Phys. Rev. Lett. 41, 607 (1978).

2. D. G. Crabb et al., Phys. Rev. Lett. 41, 1257 (1978).

3. K. Kuroda et al., "A Scintillation Target for the Calibration of High Energy Polarized Beams", Paper presented at the 1980 International Symposium on High Energy Physics with Polarized Beams and Polarized Targets, Lausanne, Switzerland September (1980).

4. I. P. Auer et al., Phys. Rev. Lett. 41, 354 (1978).

Figure Captions

Figure 1 Layout of total cross-section ($\Delta\sigma_L^{Tot}$) experiment.

C1: Beam Cherenkov counter

Q13-Q16: Last quadrupole string

A1 and A2: Beam anticounters

H1 and H2: Beam hodoscopes

H3-H5: Scintillator hodoscope

C2: Anti-Cherenkov counter

Figure 2 Estimated polarized proton and antiproton beam intensities.

Figure 3 Scintillation-counter hodoscope layout.

Figure 4 Electronic circuitry for hardwired logic functions.

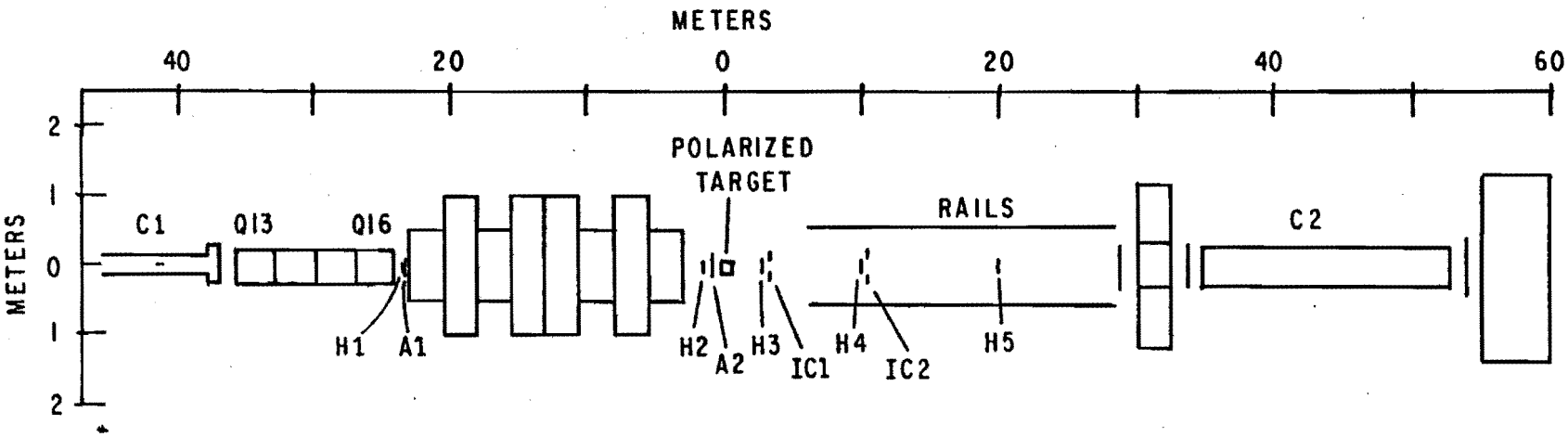
METERS
40
20
0
20
40
60
2
1
0
1
2
METERS
POLARIZED
TARGET
C1
Q13
Q16
RAILS
C2
H1
A1
H2
A2
H3
IC1
H4
IC2
H5

Figure 1

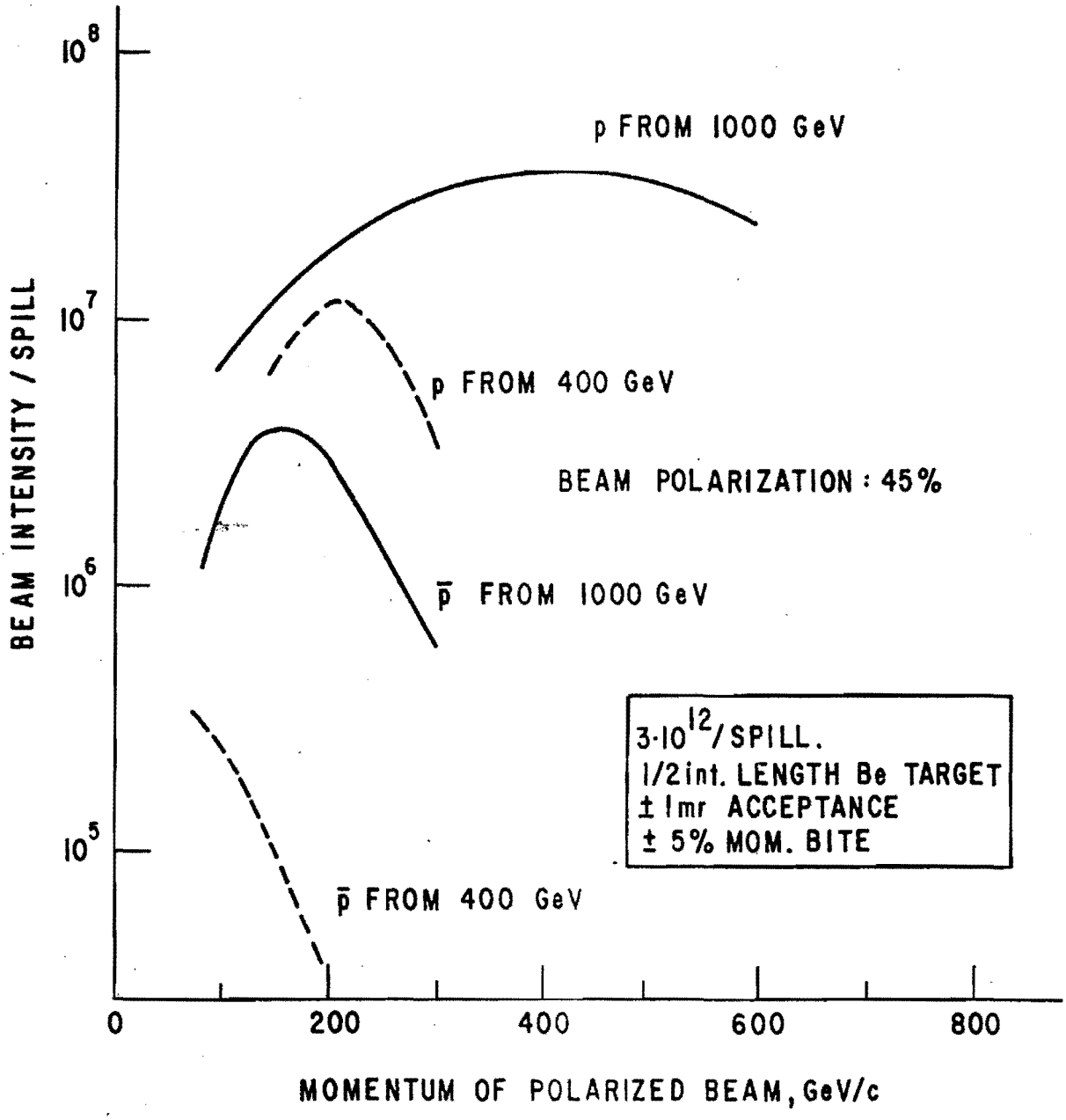
BEAM INTENSITY / SPILL
10^8
10^7
10^6
10^5
p FROM 1000 GeV
p FROM 400 GeV
BEAM POLARIZATION : 45%
$\bar{p}$ FROM 1000 GeV
$3 \cdot 10^{12}$/SPILL.
1/2int. LENGTH Be TARGET
± 1mr ACCEPTANCE
± 5% MOM. BITE
$\bar{p}$ FROM 400 GeV
0
200
400
600
800
MOMENTUM OF POLARIZED BEAM, GeV/c

Figure 2

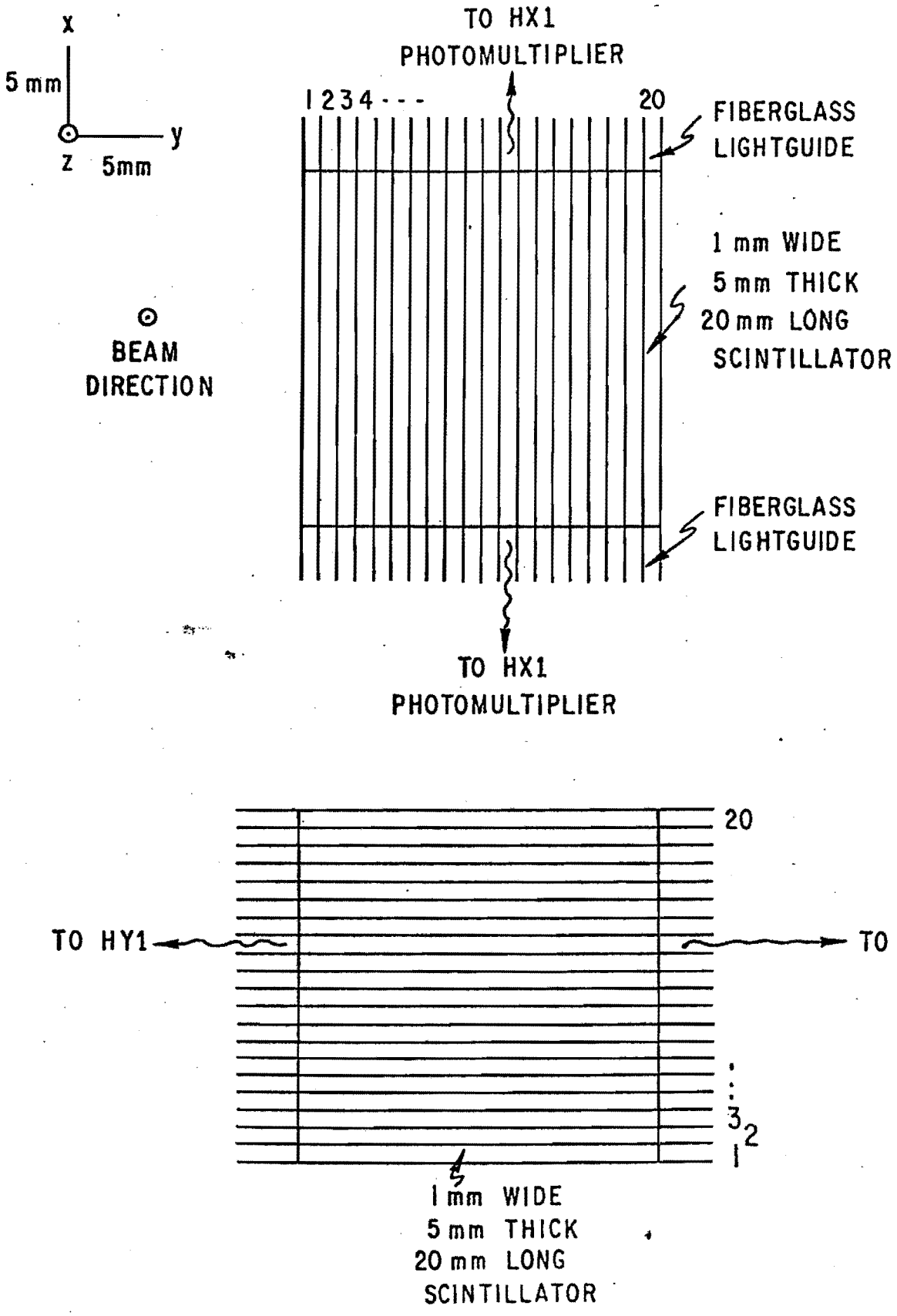
x
5 mm
y
z 5mm
TO HX1
PHOTOMULTIPLIER
1 2 3 4 - - -
20
FIBERGLASS
LIGHTGUIDE
1 mm WIDE
5 mm THICK
20 mm LONG
SCINTILLATOR
BEAM
DIRECTION
FIBERGLASS
LIGHTGUIDE
TO HX1
PHOTOMULTIPLIER
20
TO HY1
TO HY1
3
2
1
1 mm WIDE
5 mm THICK
20 mm LONG
SCINTILLATOR

Figure 3

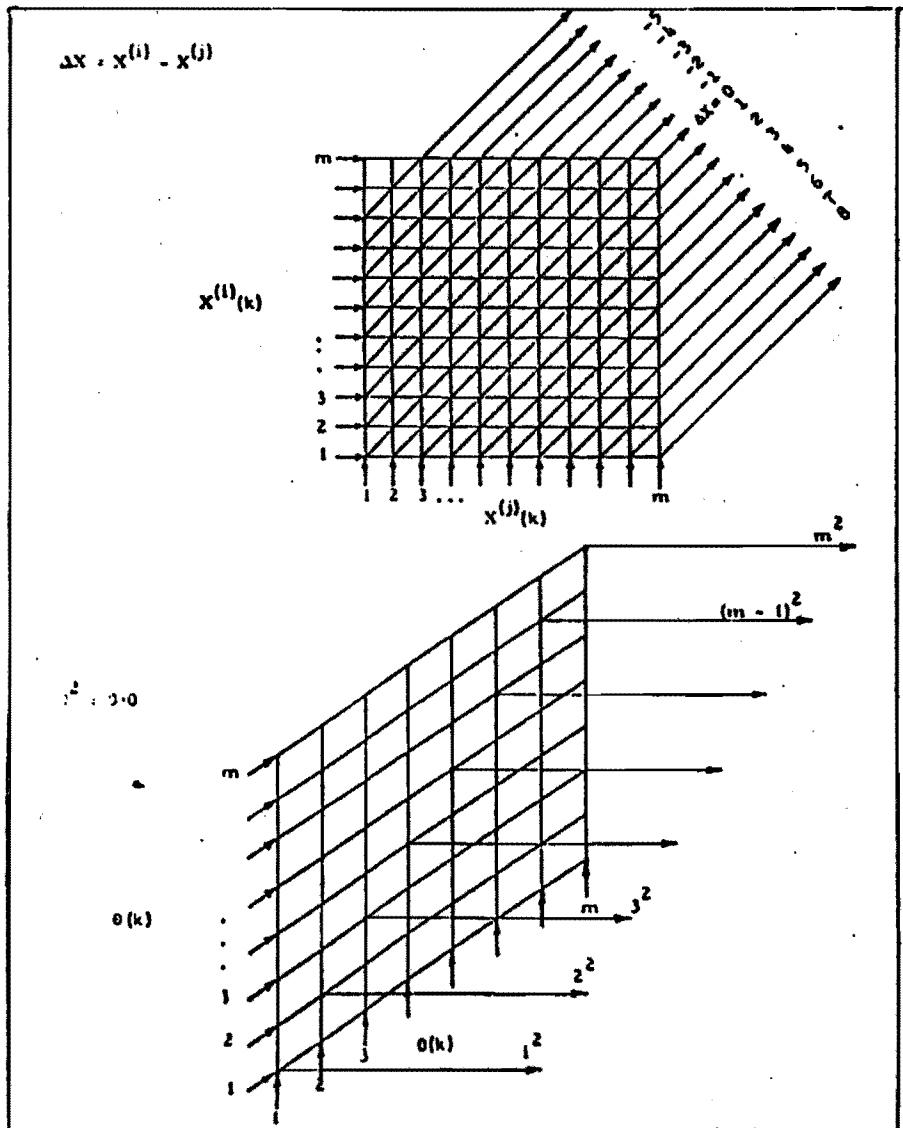

A set of n arraye ie given, each of which has m logical (0, 1) elements:

$X^{(j)}(k); \begin{pmatrix} j = 1,..,n \\ k = 1,..,m \end{pmatrix}$ e.g. $X^{(3)} = (0, 0, 1, 0, 0, 1, \ldots, 1, 0)$

Find the "true" (=1) element with the minimum k-index over all arrays.

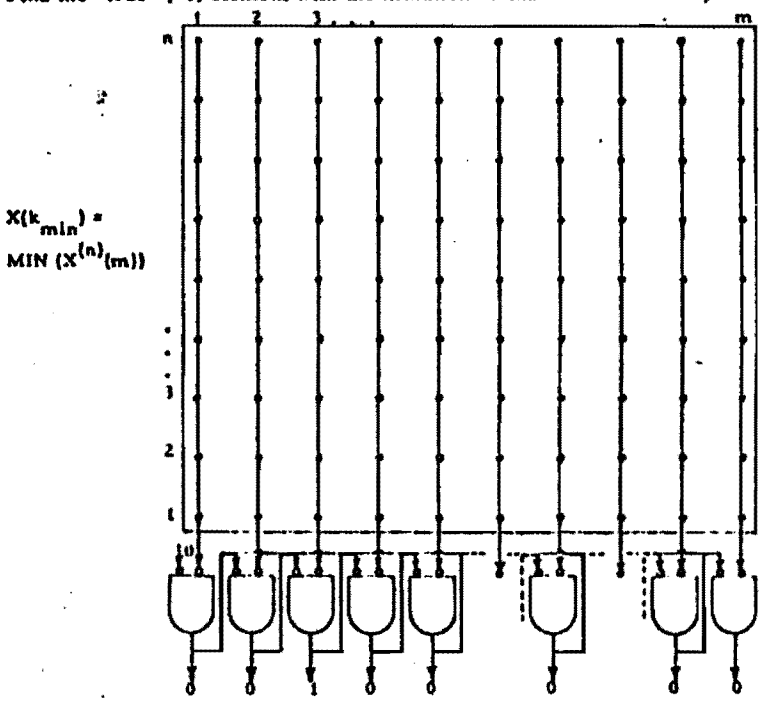

The first "1" appearing at the output suppresses all the other "1"'s
Here $k_{min} = 3$.
The sites of each matrix-row are inverted input points for the m elements of each array.
The kth vertical line corresponds to the logical "AND" of the sites of the kth column, ie. the kth elements of the n arrays.

Figure 4